Implementation Of Localized Corrosion In The Performance Assessment Model For Yucca Mountain

Vivek Jain, Bechtel SAIC Corp. LLC, 1180 Town Center Dr., Las Vegas, NV, 89144, vivek_jain@ymp.gov

S. David Sevougian, Sandia National Laboratories, P.O. Box 5800, Albuquerque, NM 87185

Patrick D. Mattie, Sandia National Laboratories, P.O. Box 5800, Albuquerque, NM 87185

Kevin G. Mon, Framatome ANP, Inc., 1180 Town Center Dr, Las Vegas, NV, 89144, and

Robert J. Mackinnon, Sandia National Laboratories, P.O. Box 5800, Albuquerque, NM 87185

AAbstractC@ *A total system performance assessment (TSPA) model has been developed to analyze the ability of the natural and engineered barriers of the Yucca Mountain repository to isolate nuclear waste over the 10,000-year period following repository closure. The principal features of the engineered barrier system (EBS) are emplacement tunnels (or "drifts") containing a two-layer waste package (WP) for waste containment and a titanium drip shield to protect the waste package from seeping water and falling rock. The 20-mm-thick outer shell of the WP is composed of Alloy 22, a highly corrosion-resistant nickel-based alloy. The barrier function of the EBS is to isolate the waste from migrating water. The water and its associated chemical conditions eventually lead to degradation of the waste packages and mobilization of the radionuclides within the packages. There are five possible waste package degradation modes of the Alloy 22: general corrosion, microbially influenced corrosion, stress corrosion cracking, early failure due to manufacturing defects, and localized corrosion. This paper specifically examines the incorporation of the Alloy-22 localized corrosion model into the Yucca Mountain TSPA model, particularly the abstraction and modeling methodology, as well as issues dealing with scaling, spatial variability, uncertainty, and coupling to other sub-models that are part of the total system model.*

I. INTRODUCTION

The geologic disposal of radioactive waste at Yucca Mountain is based on multi-barrier system, which is comprised of natural barriers and engineered barriers to contain and isolate the waste. The total system performance assessment (TSPA) model was developed to analyze the ability of these barriers to isolate nuclear waste for the 10,000-year period following repository closure. Characteristics of the natural system at Yucca Mountain that aid in repository performance include a semiarid climate, relatively stable site geology, a deep water table, and unsaturated and saturated zones which are part of a closed hydrologic basin in a desert surface environment. The principal features of the engineered barrier systems (EBS) are a titanium drip shield and a two layer waste package (WP) used for waste containment. The barrier functions of the EBS are to isolate the waste forms from the migrating water and chemical conditions leading to mobilization of the radionuclides. The waste package degradation is analyzed for various degradation modes in response to coupled thermal, hydrologic, chemical and mechanical processes in the EBS. These modes include general corrosion (GC), localized corrosion (LC), and stress corrosion cracking.

II. LOCALIZED CORROSION OF ALLOY 22

The outer barrier of the YM waste packages (WP) is made up of Alloy 22 (UNS N06022) which consists, by weight, of 20.0 to 22.5% chromium, 12.5 to 14.5% molybdenum, 3.5% tungsten, 2.0 to 6.0% iron, 2.5% (maximum) cobalt, and the balance nickel (i.e., about 50% nickel) and is highly resistant to corrosion. The unusual corrosion resistance of Alloy 22 is mainly due to addition of molybdenum and chromium to the nickel base (Hack 1983), which stabilizes the passive metal oxide film on exposed surfaces, making Alloy 22 highly resistant to general and localized corrosion (LC). Localized corrosion is a phenomenon in which corrosion progresses at discrete sites or in a nonuniform manner. Although the alloy forms relatively stable oxide films (passive films), which impede the rate of electrochemical reactions, under aggressive environmental exposure conditions, the passive films may breakdown locally (typically at defect sites in the film) leading to localized attack of the underlying alloy. The rate of localized corrosion is generally much higher than the rate of general corrosion. For YM EBS modeling the dominant form of LC is assumed to be crevice corrosion rather then pitting corrosion, because initiation thresholds for crevice corrosion of Alloy 22 in terms of water chemistry and temperature are lower than for pitting corrosion (Gdowski 1991).

The Alloy 22 outer barrier experiences a wide range of exposure conditions, primarily due to varying chemistry and temperature, which affect the localized corrosion process. Crevice corrosion may occur under a variety of conditions potentially conducive to forming tight crevices, such as (1) mineral deposits on the Alloy 22 surface left from the evaporation of the seeping water, (2) contact areas between fallen rock and the Alloy 22 waste package outer surface, and (3) contact areas between the emplacement pallet on which the package rests and the Alloy 22 outer surface. The area between the inner stainless steel vessel and the outer Alloy 22 vessel of each waste package could also be considered a crevice after the outer layer is breached. The chemical environment in a creviced region may be more severe than the EBS near-field environment due to hydrolysis of dissolved metals in the crevice. Metal ion hydrolysis can lead to the accumulation of hydrogen ions and a corresponding decrease in pH. Electromigration of chloride ions (and other anions) into the crevice must occur to balance the charge within the crevice (Jones 1992, Chapter 7), leading to a migration of positively charged metal ions (i.e., corrosion).

Localized corrosion of Alloy 22 is analyzed with two model components: an initiation model and a propagation model. In the initiation model, localized corrosion occurs when the open-circuit potential, or corrosion potential (E_{corr}), is equal to or greater than a critical threshold potential ($E_{critical}$), that is, ΔE (= $E_{critical} - E_{corr}$) ≤ 0. The magnitude of ΔE is an index of the localized corrosion resistance. The larger the positive difference, the greater is the localized corrosion resistance. This conceptual model of localized corrosion initiation is widely accepted by the corrosion community and has been published extensively (e.g., Böhni 2000). Exposure condition parameters important to corrosion are the temperature and composition of the solution contacting the metal, which include hydrogen ions (pH), halide ions (e.g., chloride ions), and corrosion-inhibiting ions (e.g., nitrate ions). LC requires the presence of a liquid water film on the WP surface. In YM this water is the dripping seepage water that contacts the WP after draining by gravity through the crown of the emplacement tunnels. The $E_{critical}$ can be defined as a certain potential above which the current density or corrosion rate of Alloy 22 increases irreversibly above the general corrosion rate of the passive metal and, therefore, represents local breakdown of the passive film that would normally protect the material from crevice corrosion. The "true" value of $E_{critical}$ for a metal or alloy, for a given set of conditions, is considered to be the lowest potential at which the corrosion current, when held potentiostatically, does not decay with time and stays above the passive current density. The crevice repassivation potential (E_{rcrev}) is used to obtain the critical potential for the initiation of LC and is determined by evaluating the current as the electrochemical potential is continuously scanned from the open-circuit or corrosion potential following a relatively short period of exposure of the metal specimen to the environment. At the breakdown potential the current experiences a sharp increase, indicative of the breakdown of the passive film. The repassivation point is determined by reversing the potential scan and noting when the reverse current scan crosses the forward current scan (In the potential scan shown in Figure 1, the repassivation point/potential is designated as E_R).

The model for E_{rcrev} was developed using a regression model fit to experimental cyclic polarization data. The regression model relates corrosion potential to the major exposure-environment variables: temperature, pH, chloride ion concentration, and nitrate ion concentration. The crevice repassivation potential, E_{rcrev}, is expressed as

$$E_{rcrev} = E^{o}_{rcrev} + \Delta E^{NO_3^-}_{rcrev} \qquad \text{(Eq. 1)}$$

where E^{o}_{rcrev} is the crevice repassivation potential in the absence of inhibitive nitrate ions, and $\Delta E^{NO_3^-}_{rcrev}$ is the crevice repassivation potential changes resulting from the

inhibiting effect of nitrate in solution. E^{o}_{rcrev} is defined in terms of WP surface temperature and chemical conditions as follows (BSC, 2004):

$$E^{o}_{rcrev} = a_o + a_1 T + a_2 pH + a_3 log([Cl^-]) + a_4 T log([Cl^-])$$

(Eq. 2)

where a_o, a_1, a_2, a_3, and a_4 are uncertain regression constants coupled with a covariance matrix, T is the WP outer surface temperature (°C), pH is the negative log of the hydrogen ion activity, and $[Cl^-]$ is the chloride ion molality (moles/kg water). The effect of nitrate ion concentration on the crevice repassivation potential is represented as

$$\Delta E^{NO_3^-}_{rcrev} = b_o + b_1[NO_3^-] + b_2 \frac{[NO_3^-]}{[Cl^-]} \quad \text{(Eq. 3)}$$

where b_o, b_1, and b_2 are constants, $[NO_3^-]$ is the nitrate ion molality (moles/kg water), and $[Cl^-]$ is the chloride ion molality. As indicated in the above equation, the effect of the interaction of the competing aggressive chloride ions and the inhibitive nitrate ions on the crevice repassivation potential is represented through the ratio of the concentrations of the two competing ions and the concentration of the nitrate ion. The ratio term is limited to a value of 0.5.

The long-term steady-state corrosion potential, E_{corr}, for the WP outer surface is expressed as

$$E_{corr} = c_o + c_1 T + c_2 pH + c_3[Cl^-] + c_4 \log(\frac{[NO_3^-]}{[Cl^-]}) \quad \text{(Eq. 4)}$$

where c_o, c_1, c_2, c_3, and c_4 are uncertain regression coefficients of the parameters, and the other parameters are as previously defined.

The other localized corrosion model component as mentioned above, is the propagation model. For Yucca Mountain EBS modeling a constant (time-independent) penetration rate after LC is initiated is assumed. Although this penetration rate is modeled as time invariant, the true crevice corrosion propagation rate would be expected to decrease with time and increasing depth of the crevices under realistic conditions.

III. IMPLEMENTATION OF LOCALIZED CORROSION IN TSPA

Modeling of the localized corrosion degradation process requires characterization of the flow rate and chemistry of the seeping water into the emplacement drifts. Decay heat from the radioactive waste forms will heat the water to temperatures above boiling for close to 1000 years after repository closure. When the water eventually condenses and drips onto the waste packages, there is a potential to cause localized corrosion depending on the chemistry of the heated water, for example, depending on its pH and the concentration of chloride ions. The uncertainty and spatial variability in these environmental parameters is modeled within the TSPA to give a reasonable representation of the expected evolution of the EBS.

The integrated performance assessment is complicated by the uncertainties that arise from the combination of the random nature of some events, incomplete understanding of the underlying processes, and limited data and information. These include model uncertainty, parameter uncertainty, parameter variability, and uncertainty in future events. Aleatory uncertainty refers to inherent unpredictability and randomness in the repository system and is considered to be irreducible. At Yucca Mountain, the major source of this uncertainty arises from the occurrence of disruptive events (i.e., those associated with igneous or seismic activity). For example, although additional study may be conducted to improve the characterization of aleatory uncertainty, this uncertainty cannot be removed through such study. Epistemic uncertainty arises from a lack of knowledge about parameters and models, which can be reduced by additional testing and data collection. The spatial and temporal scale variabilities arise from the heterogeneity or vaiability in processes and parameters at the spatial-temporal scales. These aleatory and epistemic uncertainties are accounted for in the LC initiation model with probabilistic Monte Carlo simulations based on multiple realizations of the probability distributions representing these various forms of uncertainty and variability.

The TSPA model implementation of LC is done in two sequential parts: (1) the LC initiation analysis that evaluates the chemical conditions for LC initiation on the WP outer surface and (2) the LC submodel within the overall TSPA model, which calculates WP failure histories based on the chemistry evaluation from the LC initiation analysis and on the sampled values of the localized corrosion and general corrosion propagation rates. Figure 2 shows the key EBS submodels or inputs to the LC initiation analysis:

- EBS Chemical Environment Submodel: Used for evolution of carbon dioxide fugacity in the gas phase and evolution of the dissolved ion concentrations (e.g.,

nitrate, chloride, pH) in the liquid phase of the seepage water dripping onto the waste package. These evolve in response to the thermal decay pulse from the hot waste packages.

- Drift Seepage Submodel: Used to determine the magnitude and location of seepage water entering the emplacement tunnels.

- EBS Thermal-Hydrology (TH) Environment Submodel: Provides time-dependent values for temperature and relative humidity on WP surfaces and drift-wall temperature. The sub-model abstraction also provides time-dependent adjusted values that are used to correct temperature and relative humidity values for the insulating effect of rubble caused by drift degradation induced by seismic ground motion.

- LC Initiation Analysis: Determines ΔE as a function of time based on the chemical and thermal time histories, and subsequently outputs an indicator variable, I, to record whether a waste package has a favorable (I = 1) or unfavorable (I = 0) for localized corrosion initiation.

The LC initiation analysis includes two computational loops: an outer epistemic uncertainty loop, and an inner spatial variability loop. In the outer loop, Monte Carlo sampling is performed on 24 uncertain epistemic parameter distributions, including the LC initiation model regression coefficients (a_0, a_1, a_2, a_3, a_4, c_0, c_1, c_2, c_3, and c_4) associated with the crevice repassivation potential and the long-term steady-state corrosion potential, the chemical environment parameters on the WP outer surface (i.e., pH, nitrate concentration, chloride concentration), seepage water flux (fracture permeability and capillarity), and the thermal conductivity of the rubble backfill caused by a seismic event.

The inner or spatial variability loop is based on a highly discretized thermal-hydrology model, which divides the repository into thousands of equal-area subdomains and calculates the temperature and relative humidity time histories for several waste package types with different heat outputs within each subdomain, including both commercial spent nuclear fuel (CSNF) waste packages and co-disposal (CDSP) waste packages (which contain both defense high-level waste glass and defense spent nuclear fuel). Parameters sampled in the inner spatial variability loop are drift-seepage parameters including the flow focusing factor, spatial variability of fracture permeability, and capillarity at each of the subdomains.

It is important to correctly capture this thermal-hydrologic (TH) heterogeneity to accurately represent the LC initiation analysis. For Yucca Mountain EBS modeling, the multiscale thermal hydrology (MSTH) Model is used to predict spatial variability in TH response across the repository. In particular, this model subdivides the repository footprint into 2,874 equal-area subdomains. For epistemically uncertain infiltration conditions, the MSTH Model calculates time-dependent TH variables (temperature and relative humidity) for six representative CSNF and two representative CDSP waste packages and drip shield (DS) pairs at each subdomain location. The percolation flux at each of the 2,874 MSTHM Process Model subdomain locations are used to group the subdomain locations into 1 of 5 repository percolation subregions (Figure 3). The MSTHM Abstraction produces two sets of outputs that are indexed by fuel type (CSNF and CDSP) and percolation subregion (1 to 5). The LC analysis is done for all of these sets individually as shown in Figure 4, and described below.

A Monte Carlo sample set (Latin hypercube sampling, LHS) of sufficient size, N_{LC} = 100, is used to evaluate the 24 epistemic uncertainties (outer loop). After the epistemic parameters are sampled, the simulation is broken into 50 different cases with the Monte Carlo sample set applying equally to all 50 cases. These 50 (5 x 5 x 2 = 50) cases are a combination of (1) coarse-scale spatial heterogeneity (the five percolation subregions shown in Figure 3); (2) five thermal-hydrologic cases (low-low, low-mean, mean-mean, high-mean, and high-high) representing coarsely discretized epistemic uncertainty in percolation flux (low, mean and high) and host-rock thermal conductivity (low, mean and high); and (3) the packaging of the waste into CSNF and CDSP packages. Next, for each outer-loop realization (R_{LC} = 1, 2, ..., N_{LC}) and for each of the 50 cases an inner loop over all the N_{SL} locations in the percolation subregion is executed (N_{SL} is a subset of the 2874 subdomains, e.g., Subregion 3, the largest of the five percolation subregions, encompasses 1151 of the 2874 subdomains). Spatially variable parameters, which include temperature and relative humidity time histories, flow focusing factor, fracture permeability, and capillarity, associated with one of the six CSNF WP or one of two CDSP WP at each of the 2874 subdomains are sampled in the inner loop. For example, subregion 3 will have 100 (N_{LC}) × 1151 (N_{SL}) = 115,100 realizations of localized corrosion analysis. Similarly rest of the subregions (1,2, 4 and 5) with lesser number of subdomains will have smaller number of total realizations in each case. The output generated is primarily the time histories of LC initiation (represented by a sequence of zeroes and ones as shown in Figure 2) due to the chemical evolution of crown seepage water on each of the N_{SL} WPs in the percolation subregion.

IV. RESULTS

Figure 5 shows the LC initiation analysis under given sets of environmental (chemical) conditions as a function of temperature, over the ranges of uncertainty in the LC initiation model regression coefficients (a_0, a_1, a_2, a_3, a_4, c_0, c_1, c_2, c_3, and c_4). As demonstrated in Figure 5, if there is water film present on the WPs with the following chemistry inputs: pH = 7, chloride concentration = 10 molal, and nitrate concentration = 1.5 molal, then over the temperature range of 30°C to 120°C, LC initiation occurs above 110°C for the mean values of E_{corr} and E_{rcrev}. Even though E_{corr} is greater than E_{rcrev} at these temperatures, thereby implying localized corrosion initiation, seepage water is not expected to drip on the waste packages because of the presence of drip shield. Hence there is no localized corrosion initiation expected on the Alloy 22. Similarly, Figure 6 shows that with the following chemistry inputs: pH = 3, chloride concentration = 10 molal, and a very low nitrate concentration of 0.5 molal, E_{corr} is always greater than E_{rcrev} and LC is expected to occur over the whole range of temperatures: 30°C to 120°C, if seepage occurs. However these conditions are not expected in the repository.

In the TSPA model the output generated from the LC initiation analysis is used in the LC submodel to determine the number of packages that will experience localized corrosion, based on the timing of a seismic event or other condition that can fail the drip shield and expose the waste package to seeping water. Based on the current repository design and the evolution of THC processes in the natural barriers, preliminary analyses show a low probability of localized corrosion having a significant impact on EBS performance. For example, the presence of a thermal barrier during the initial years (when the temperature is high) and the presence of the drip shields prevent seepage water from contacting the waste packages, thereby limiting waste package degradation due to localized corrosion.

V. CONCLUSION

The localized corrosion model incorporates a wide range of conditions, primarily due to varying chemistry and temperature on the waste package Alloy 22 outer barrier. The model incorporates spatial variability and uncertainty in the different submodels affecting localized corrosion initiation. The uncertainties are sampled for multiple realizations that generate a response surface, which is integrated in the TSPA model to determine the number of waste packages that will experience localized corrosion. The coupling of the LC submodel within the TSPA model is complex because of the numerous processes involved, including seepage, thermal-hydrology, thermal-hydrology-chemistry (THC), seismic, drift-degradation, and general corrosion processes. However, by using various levels of discretization for uncertainty and variability as appropriate to the processes involved the problem is implemented in a multi-realization, Monte Carlo performance assessment model.

VI. ACKNOWLEDGEMENTS

We would like to thank other scientists on the Yucca Mountain Project for contributions to the text of this paper, including Peter Swift, Cedric Sallaberry, Bryan Bullard, Bryan Dunlap, Pat Lee, Tom Buscheck, Jerry McNeish, Ralph Rogers, Debbie Miller et. al.

V. REFERENCES

1. Hack, H.P. "Crevice Corrosion Behavior of Molybdenum-Containing Stainless Steels in Seawater." *Materials Performance, 22*, (6), 24-30. Houston, Texas: NACE International. TIC: 245826, (1983.)

2. Gdowski, G.E. "*Survey of Degradation Modes of Four Nickel-Chromium-Molybdenum Alloys*. UCRL-ID-108330". Livermore, California: Lawrence Livermore National Laboratory. ACC: NNA.19910521.0010, (1991).

3. Jones, D.A. "*Principles and Prevention of Corrosion.*" 1st Edition. New York, New York: Macmillan, (1992).

4. Böhni, H. "*Localized Corrosion of Passive Metals.*" Chapter 10 of *Uhlig's Corrosion Handbook*. Revised, R.W., ed. 2nd Edition. New York, New York: John Wiley & Sons, (2000).

5. Payer, J.H. "*Corrosion Resistance of Alloy 22*". Presented to: Nuclear Waste Technical Review Board, May 18-19, 2004. Washington, D.C.: U.S. Department of Energy, Office of Civilian Radioactive Waste Management. ACC: MOL.20040629.0421 (or http://www.nwtrb.gov/meetings/may%202004/payer.pdf)

6. BSC. "*General Corrosion and Localized Corrosion of Waste Package Outer Barrier*". ANL-EBS-MD-000003 REV 02. Las Vegas, Nevada: Bechtel SAIC Company. ACC: DOC.20041004.0001 (2004).

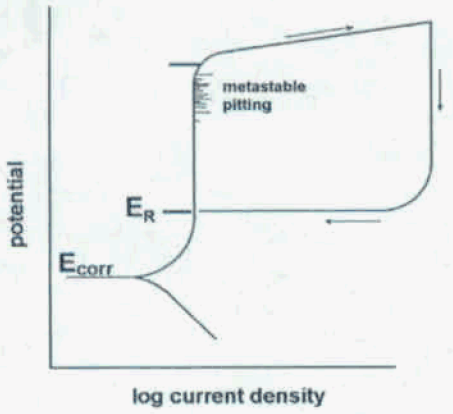

Figure 1. Example of a Cyclic Potentiodynamic Polarization Scan for Alloy 22 (after Payer 2004)

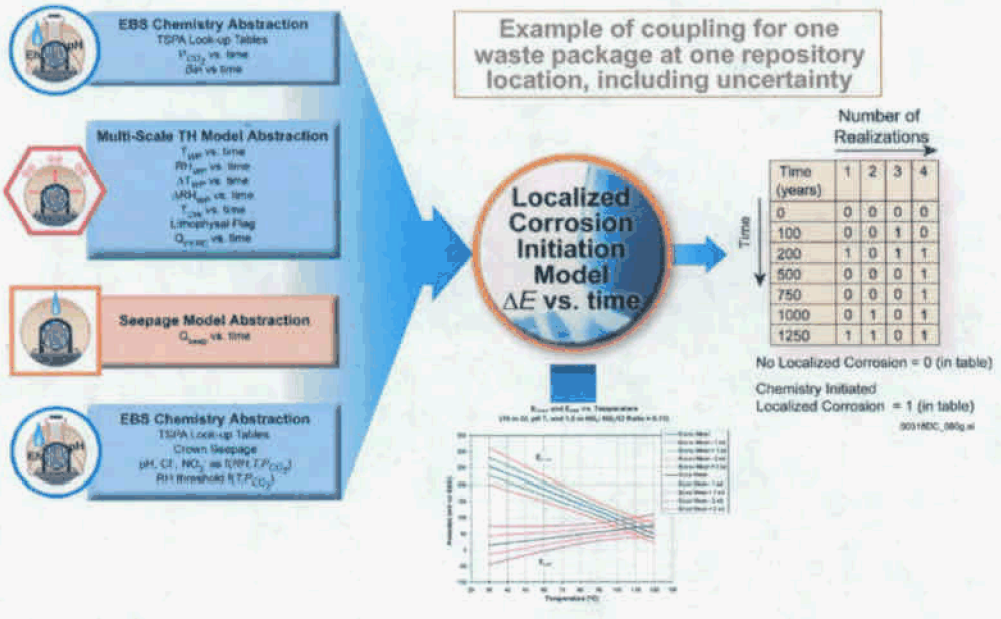

Figure 2. Coupling of EBS Localized Corrosion Initiation Model with Environmental Input Models and Abstractions

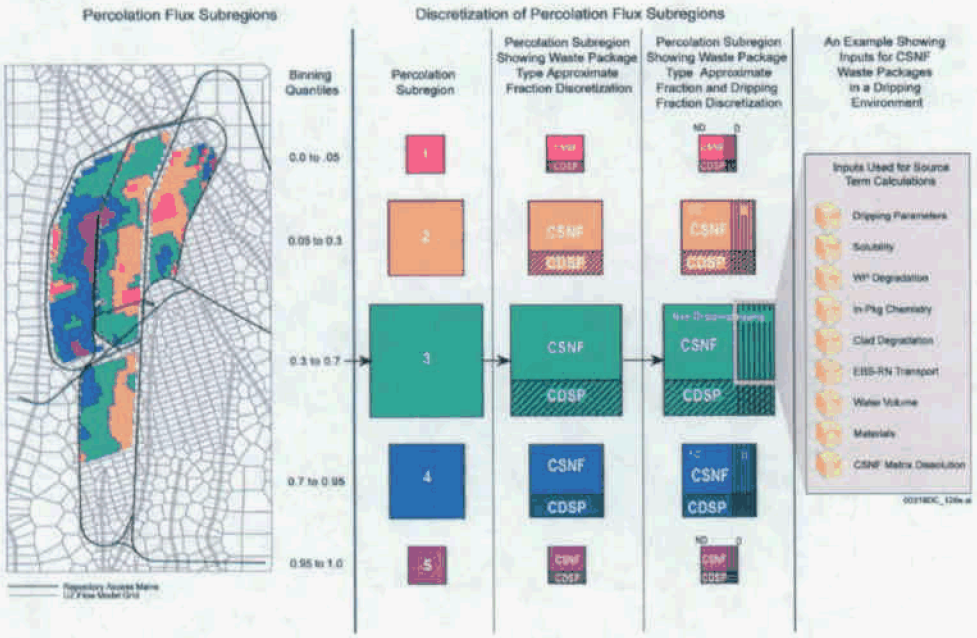

Figure 3. Spatial Scales and Levels of Discretization in the TSPA EBS Model Suite

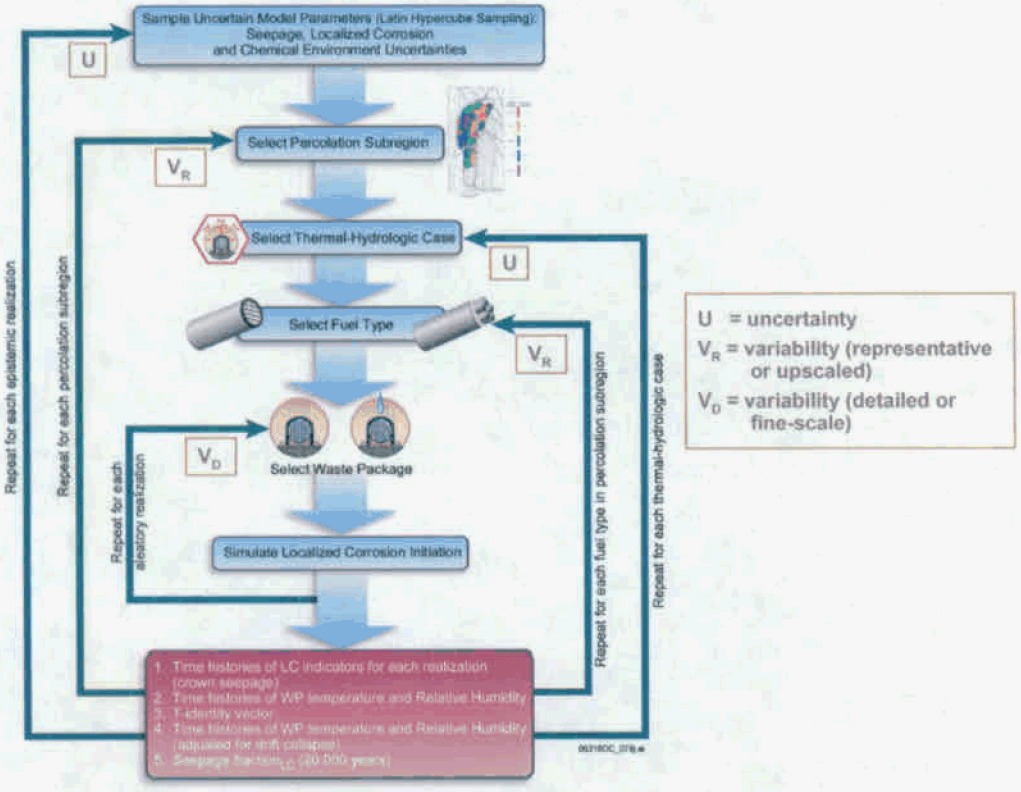

Figure 4. Implementation and Connection of the Localized Corrosion Initiation Model, and Associated Uncertainties and Variabilities, into EBS and Total System Modeling

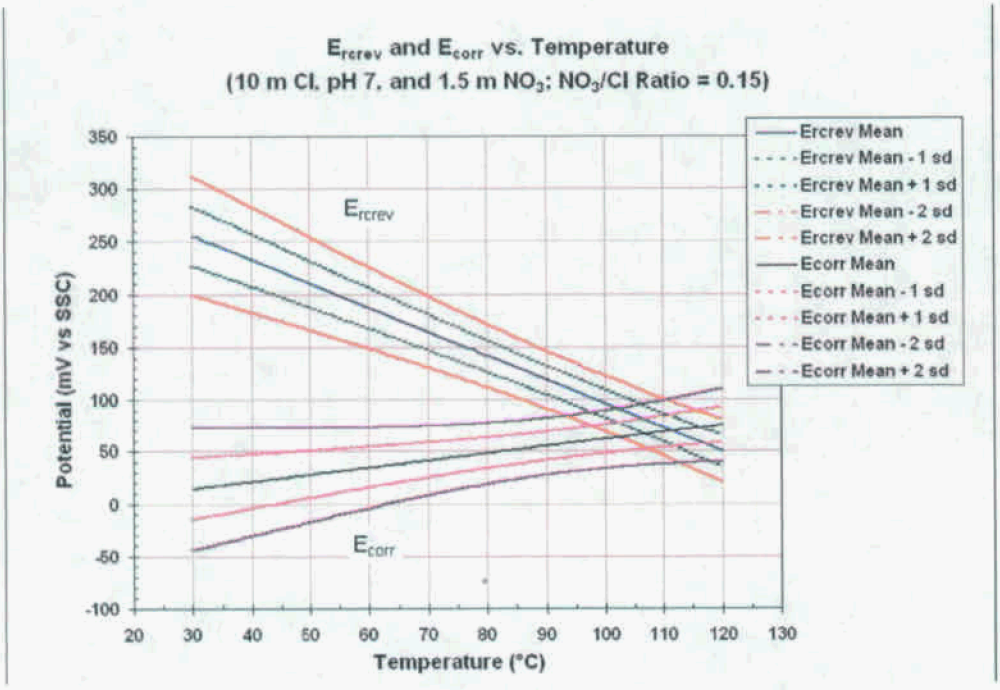

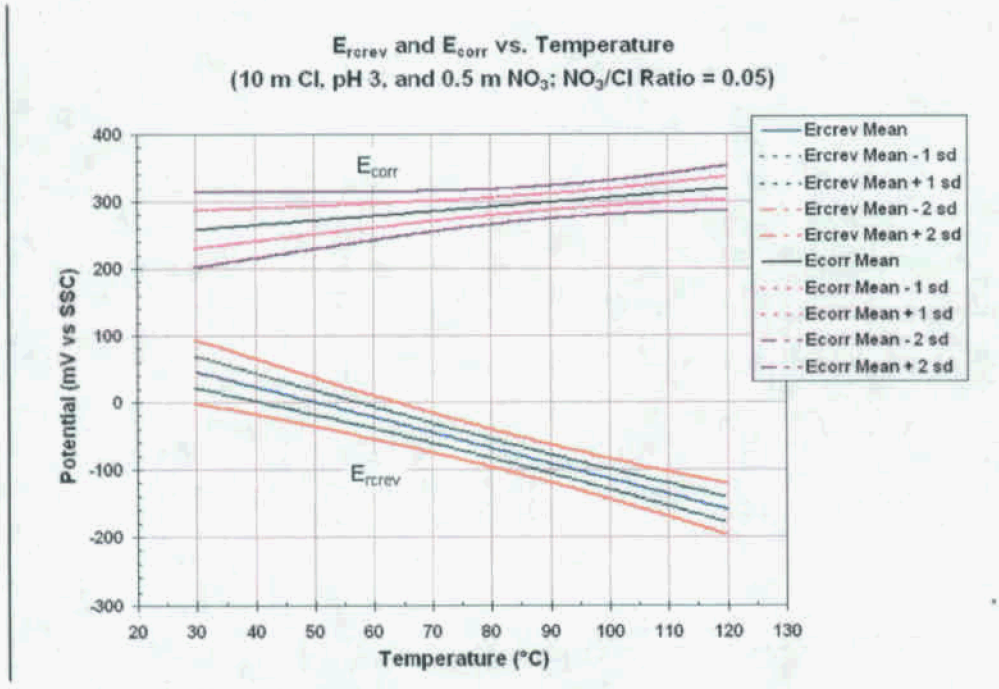

Figure 5. Example results of Localized corrosion analysis at a fixed chemistry input to the model with their associated uncertainties.